THREE-DIMENSIONAL LIGHTNING LOCATION RELATIVE TO STORM STRUCTURE IN A MESOSCALE CONVECTIVE SYSTEM

Lawrence D. Carey[1*], Martin J. Murphy[2], Tracy L. McCormick[3], and
Nicholas W. S. Demetriades[2]

[1]*Texas A&M University, College Station, TX*

[2]Vaisala, Tucson, AZ

[3] National Weather Service, Boston Forecast Office, Taunton, MA

1. INTRODUCTION

Mesoscale convective systems (MCSs) produce a significant fraction of the warm season rainfall, lightning, and severe weather in the central United States [e.g., Fritsch et al., 1986; Goodman and MacGorman, 1986; Houze et al., 1990]. As a result, the concomitant kinematic, microphysical, electrical, and lightning characteristics of MCSs over this region have received considerable research attention [e.g., Houze, 1993; MacGorman and Rust, 1998; Fritsch and Forbes, 2001].

Nearly all studies of lightning in MCSs have analyzed exclusively ground flashes in relation to storm structure [e.g., MacGorman and Rust, 1998 for a review]. One notable exception is Mazur and Rust [1983], who observed the total lightning structure roughly perpendicular to what appeared to be a leading-line, trailing-stratiform (LLTS) MCS with radar. Total lightning flash density in the stratiform region was typically much smaller than in the convective cells. Lightning possessing radial extent in excess of 20 km tended to occur rearward of the deep convective cells and in the stratiform region. Since their lightning observations were limited to a radar beam that was approximately fixed in elevation and azimuth angle, only a two-dimensional view of mid-level precipitation and lightning flash density could be obtained as the MCS moved toward the radar (i.e., range versus time). More recently, Lyons et al. [2003] examined the vertical profile of VHF sources associated with fifteen sprite-producing positive cloud-to-ground (CG) lightning flashes in the stratiform region of an MCS. The average height of VHF sources associated with sprite-producing ground flashes was consistently at low levels in the stratiform region near the melting level at about 4.1 km AGL. Lang et al. [2004a] examined the origins of 39 stratiform region CG lighting flashes in a small, asymmetric LLTS MCS. Thirty (77%) of the stratiform region ground flashes were initiated in the leading convective line, while the remainder initiated in the stratiform region. In each of these studies, information

on total lightning location within LLTS MCSs was limited either in scope (e.g., sprite producing positive CG flashes only; origins of positive CG flashes) or in spatial dimension (e.g., vertical profile or quasi-horizontal plan view). Other studies have focused on the three dimensional lightning structure of "spider lightning" within the stratiform anvils of decaying, weakly organized convection [e.g., Boccippio, 1996; Mazur et al., 1998]. Although there may be some similarities between the dynamics, microphysics, and lightning structure of stratiform regions within weakly organized, dissipating convection and that within highly organized LLTS MCSs, it is unclear at this time how far the analogy can be taken. Since there are well known differences in the mesoscale environment and dynamics of these storms [e.g., Houze, 1993], we believe that caution must be exercised in drawing comparisons and further analysis in both storm types is warranted.

Recently, lightning networks measuring the time of arrival of impulsive VHF (very high frequency) radiation using GPS (Global Positioning System) timing have been developed that provide an accurate and detailed depiction of three-dimensional lightning structure [Rison et al., 1999]. Results from these networks have provided an unprecedented view of lightning within isolated convection, multicell storms, and supercells [Rison et al., 1999; Krehbiel et al., 2000; Coleman et al., 2003]. Lyons et al. [2003] and Lang et al. [2004a] used the same technology to examine limited characteristics of positive ground flashes within the stratiform region of LLTS MCSs during STEPS (Severe Thunderstorm Electrification Precipitation Study) [Lang et al. 2004b].

Herein, we report on unique observations of the total (i.e., both in-cloud (IC) and CG) lightning structure of a symmetric LLTS MCS [Houze et al., 1989] recorded by the Vaisala Dallas-Fort Worth (DFW) Lightning Detection and Ranging (LDAR II) research network on 16 June 2002. The VHF derived three-dimensional composite lightning structure was placed in the context of the DFW Weather Surveillance Radar 1988 Doppler (WSR-88D) (or KFWS) composite reflectivity structure, providing a fresh perspective on lightning location within LLTS MCSs. In addition, we examine the three dimensional structure of seven NLDN-detected positive ground strokes within the stratiform precipitation using LDAR II observations. A closely related study by

---

* *Corresponding author address*: Dr. Larry Carey, Dept. Atmospheric Science, Texas A&M University, College Station Texas 77843-3150; larry_carey@tamu.edu

Dotzek et al. [2004] utilized similar KFWS radar reflectivity and LDAR II lightning data and analysis techniques to explore the total lightning structure of another LLTS MCS on 7-8 April 2002 in Texas. When combined, our study and Dotzek et al. [2004] provide a comprehensive picture of VHF-based total lightning pathways within LLTS MCSs.

2. DATA AND METHODOLOGY

We employed KFWS WSR-88D reflectivity; CG flash location, time, and polarity from the National Lightning Detection Network (NLDN: owned and operated by Vaisala) [Cummins et al., 1998]; and the time and three-dimensional location of VHF radiation sources associated with total (i.e., both IC and CG) lightning as measured by Vaisala's DFW LDAR II network for a LLTS MCS that passed directly over the network on 16 June 2002. Since positive CG lightning flashes characterized by peak currents less than 10 kA were likely associated with misidentified IC lightning, they were removed from our data sample [Cummins et al. 1998; Wacker and Orville 1999a,b].

This study used KFWS level-II WSR-88D archive data (digital base data in polar format) [Crum et al., 1993] on 16 June 2002 for a 30-minute period from 0609 to 0639 UTC, while a large portion of a LLTS MCS was within 100 km of the DFW LDAR II network (Figure 1). During this period, a portion of the convective line, transition zone, and stratiform region passed over the interior of the seven-sensor LDAR II network. The KFWS radar was located approximately 44 km to the southwest of the center of the LDAR II network (Figure 1).

In this study, we used the three-dimensional LDAR II VHF lightning source data for the same 30-minute period on 16 June 2002. Using the three-dimensional location (longitude, latitude, Z) and time (T) of each LDAR II VHF radiation source, we first determined the KFWS-relative VHF source location in (X, Y, Z) and then calculated the VHF lightning source density (km^{-3} min^{-1}) at each grid point in the transformed, line-parallel versus line-normal MCS-relative coordinate system (X′, Y′, Z) for each five minute period centered on the start of each radar volume time.

Conceptual models of the microphysics and kinematics [Houze et al., 1989] and also the electrical structure [e.g., Stolzenburg et al., 1994; 1998] for the archetypal LLTS MCS have often been developed using two-dimensional, line-normal composites of many observations from a single or multiple like LLTS MCSs. The compositing approach is also pragmatic because it allows the development of a model with limited observations. For these reasons, we chose to create several two-dimensional composites of radar reflectivity and VHF lightning source density from 30 minutes of data on 16 June 2002 (0609 – 0639 UTC), while a portion of the LLTS MCS passed directly over the DFW LDAR II network. In order to adequately address the three-dimensional lightning structure within a LLTS MCS, three different types of two-dimensional composites were actually created: 1) a horizontal

composite in the line-parallel versus line-normal directions (X′-Y′), 2) a vertical composite in the line-normal direction (X′-Z), and 3) a vertical composite in the line-parallel direction (Y′-Z).
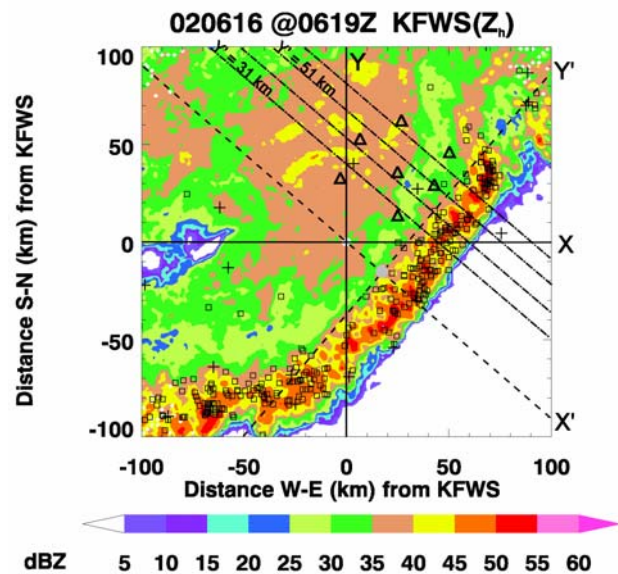

Figure 1. Low-level (2 km) horizontal cross-section of KFWS radar reflectivity (shaded as shown, dBZ) that depicts a leading-line, trailing-stratiform MCS on 16 June 2002 at 0619 UTC. Positive (negative) polarity CG flashes are indicated by plus (box) symbols for a five-minute period centered on the radar time. The triangles indicate the seven-sensor locations in the LDAR II network. The solid lines depict the original south-north (Y) versus west-east (X) coordinate system with an origin at the KFWS radar. The dashed lines depict the line-parallel (Y′) versus line-normal (X′) coordinate system, which was obtained after rotating and shifting the data from the X-Y system. The origin in the X′-Y′ coordinate system is indicated by a grey circle. The dash-dot lines indicate the planes of the vertical cross-sections (X′-Z) depicted in Figure 3.

3. RESULTS

3.1 Cloud-to-ground Lightning and Low-level Horizontal Radar Structure

The relationship between NLDN detected CG flash location, polarity, and horizontal storm structure is depicted in Figure 1 for the LLTS MCS on 16 June 2002 at 0619 UTC. This case exhibited a typical low level horizontal radar reflectivity structure. System motion was roughly perpendicular to the orientation of the convective line, or toward the southeast (130°) at 21 m s^{-1}, as expected for a LLTS MCS. Convective cells within the leading line were characterized by moderate to high values of reflectivity (40 – 55 dBZ) and were distributed uniformly along the line within the analysis domain. Consistent with the life cycle of a convective cell, which begins near the front of the convective line, the highest reflectivity tended to be associated with the developing-to-mature cells in the forward-to-center

portions of the line. Rearward of the convective line was a clear transition zone, which was characterized by a reflectivity minimum (25 – 30 dBZ) at 2 km. Reflectivity and hence precipitation rates increased again (30 – 40 dBZ) in the trailing stratiform region of the MCS. Some isolated maxima in radar reflectivity (40 – 45 dBZ) occurred in and around the LDAR II network within the stratiform region. There were some asymmetries in the convective line structure toward the extreme northeast and southwest of Figure 1. The stratiform region was not as well developed rearward of the southwest portion of the convective line.
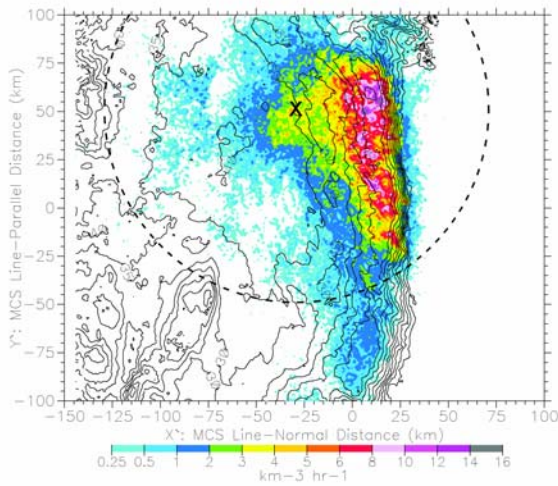
Figure 2. A 30-minute horizontal composite of radar reflectivity (dBZ, contours every 5 dBZ) at 2 km altitude and VHF lightning source density (km^{-3} hr^{-1}, shaded as shown) through the entire vertical depth of a leading line, trailing stratiform MCS over the DFW region on 16 June 2002 from 0609 to 0639 UTC. The average center of the LDAR II network during this period is indicated by the 'X' symbol. For reference, a 100 km range ring from the center of the lightning detection network is provided (dashed circle). The coordinate system for the composite is line-normal distance (X′, km) along the abscissa and line-parallel distance (Y′, km) along the ordinate. The back of the convective line (i.e., roughly the mean position of the 40 dBZ echo toward the rear) was forced to be located at X′ = 0 km as shown in Figure 1.

As in past studies [e.g., Orville et al, 1988; Rutledge and MacGorman, 1988; Rutledge et al., 1990; Stolzenburg, 1990; Holle et al., 1994; among others], the leading convective line for the MCS contained roughly an order of magnitude more CG flashes than the stratiform region (i.e., 12 times more overall) while in the vicinity of the KFWS radar (0500-0700 UTC). Ground flash locations in the convective line tended to cluster in and around convective cells with enhanced (> 45 dBZ) radar reflectivity [e.g., Toracinta et al., 1996]. Consistent with earlier studies [e.g., Orville et al., 1988; Rutledge and MacGorman 1988; Engholm et al., 1990; Stolzenburg, 1990; Rutledge et al., 1990; among

others], the MCS in our study generated a larger percentage of positive polarity CG flashes in the stratiform region (26.5 %) than in the convective line (2.0 %) during this period. Similar to MCSs studied in Rutledge and MacGorman [1988] and Rutledge and Petersen [1994], many of the positive flashes in the stratiform region clustered near local reflectivity maxima (Figure 2). As in Petersen and Rutledge (1992), the mean positive peak currents were significantly larger in the stratiform region (31.5 kA) than the convective line (22.8 kA) during this time. These peak currents are consistent with the large database of MCS peak current values compiled in MacGorman and Morgenstern [1998]. In all respects, the horizontal radar structure and CG lightning properties of the 16 June 2002 MCS were fairly typical for LLTS MCSs in the central United States and elsewhere.

### 3.2 Horizontal Radar and Total Lightning Structure

The mesoscale radar and VHF lightning source density structure were quasi-steady over the 30 minute period (0609-0639 UTC). Rather than show individual horizontal cross-sections, we chose to create a 30-minute composite of radar and VHF lightning source density structure during this period. The 30-minute horizontal composite of low-level (2 km) radar reflectivity and VHF lightning source density through the depth of the MCS was created in a line-parallel versus line-normal framework (X′-Y′) and is shown in Figure 2.

As expected, the VHF lightning sources were overwhelmingly concentrated in the convective line, with some tendency for source density maxima to occur in the rear portions of the line, as in Mazur and Rust [1983] and Dotzek et al. [2004]. More specifically, there was an order of magnitude (10 times) more VHF lightning radiation sources in the convective region compared to the stratiform region. VHF source density maxima in the convective line were well correlated with enhancements in the radar reflectivity, as in Mazur and Rust [1983] and Dotzek et al. [2004]. At ranges < 75 km (i.e., 25 - 75 km) from the center of the LDAR network, the VHF source densities in the convective line were of comparable values (3-16 km^{-3} hr^{-1}) and there was little evidence for significant range effects associated with decreasing detection efficiency with range. At distant range (> 100 km), the source densities in the convective line dropped dramatically to values between 0.25 and 2 km^{-3} hr^{-1}. This significant decrease in source densities along the convective line to the south was clearly associated with rapidly decreasing source detection efficiency with range.

In the vicinity of the LDAR II network center (X′ = -28 km, Y′ = 52 km), there was an obvious rearward extension of the VHF source density maximum from the back of the convective line in the mature-to-dissipating convection (X′ = 0 km), through the transition zone (centered at X′ = -15 km), into the stratiform region (starting at X′ = -25 km), and ending near an enhancement (> 40 dBZ) in the radar reflectivity within the middle of the stratiform region (X′ = -55 km, Y′ = 35 km). Rearward (-70 km > X′ > -100 km) of this reflectivity maximum was a separate cluster of VHF

lightning sources toward the back of the stratiform precipitation. The VHF source densities in the stratiform region south of the network interior (e.g., Y′ < 0 km) were significantly less, even though the range < 100 km. Since the stratiform region was not as well developed at Y′ < 0 km (i.e., lower values of reflectivity and less rearward extent of stratiform precipitation), it is possible that this drop off in the VHF lightning source density is associated with a decrease in the intensity and size of the stratiform region. However, the decrease is also likely associated with decreased source detection efficiency with range, meaning that the best sample of stratiform region VHF lightning source density occurred near the network center.
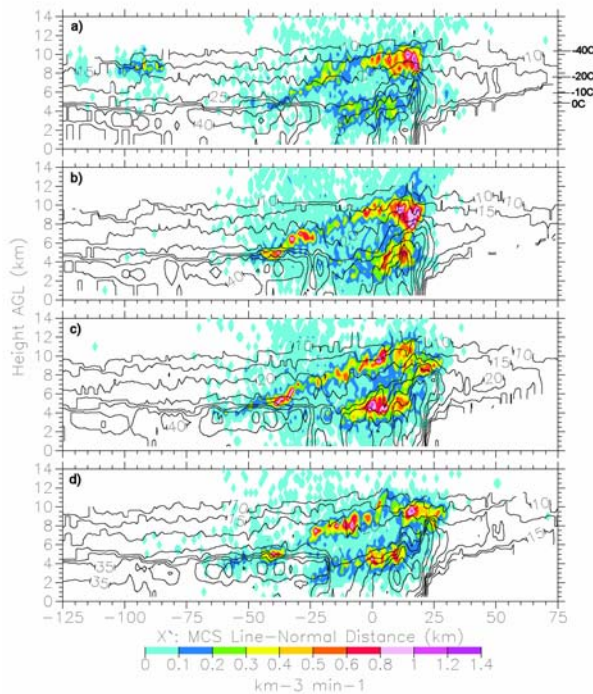

Figure 3. Line-normal (X′, km) vertical (Z, km above ground level, AGL) cross-sections of radar reflectivity (dBZ, contoured every 5 dBZ starting at 10 dBZ) and VHF lightning source density (km^{-3} min^{-1}, shaded as shown) through **a)** Y′ = 61 km, **b)** Y′ = 51 km, **c)** Y′ = 41 km, and **d)** Y′ = 31 km (see Figure 1) of a leading line, trailing stratiform MCS over the DFW region on 16 June 2002 at 0619 UTC. For each X′-Z grid box in each cross-section depicted, LDAR source density was calculated in a 10 km long cuboid along the Y′-direction that was centered on the cross-section for a five minute period centered on the radar volume time. The back of the convective line (i.e., roughly the mean position of the low-level, 40 dBZ echo) was forced to be located at X′ = 0 km as shown in Figure 1. The heights of significant temperatures (0°C, -10°C, -20°C, and -40° C), according to the FWD 00 UTC, 16 June 2002 sounding, are depicted in a).

4.3 Line-Normal Vertical Radar and Total Lightning Structure

The vertical radar and total lightning structure of the MCS at 0619 UTC are presented in a series of four vertical cross-sections in Figures 3a-d. The vertical cross-sections were taken normal (X′) to the convective line at four positions along the line (Y′ = 61, 51, 41, and 31 km) that passed through the interior of the LDAR II network, which was centered at about X′ = -25 km or toward the forward portion of the stratiform region (Figures 1 and 2).

Although there was some variability, the four cross-sections (Figures 3a-d) revealed a fairly consistent and typical (c.f. Figures 3a-d and Houze et al., 1989 or Figure 9) line-normal vertical structure of radar reflectivity. The convective line was located from about X′ = -15 km to X′ = 20 km. The 10 dBZ echo top reached up to about 12 km AGL. Newer, taller, more intense convection was located toward the front of the line. The 30 dBZ echo reached up to 8-9 km AGL there. More mature, shorter, and less intense convective echoes were located toward the rear of the line, such that the reflectivity contours slumped downward and rearward with each successively older cell. The transition zone was evident as a reflectivity minimum from near the surface to mid-levels in the MCS and was centered at about X′ = -15 km to -20 km. The radar bright band, which clearly identified the stratiform precipitation region from about X′ = -25 km to X′ = -100 km, was located at heights just below the melting level as expected. Due to the relatively coarse resolution of the KFWS WSR-88D (1° × 1 km), the reflectivity maximum associated with the bright band was smeared in the vertical such that it was about 2 to 2.5 km thick. Several reflectivity maxima of 45 dBZ were located within the broad, bright band region from about 2.5 to 4 km AGL. Above the radar bright band, precipitation structure was fairly homogeneous as expected in the stratiform region. However, there was a tendency for larger values of reflectivity to exist at a given height in the forward portions of the stratiform region. In other words, the reflectivity contours did slant downward gently with increasing distance rearward of the convective line. A prominent forward anvil was evident up to 50 km or more in advance of the convective line at heights from 4 to 12 km. According to the radar, little or no precipitation reached the ground beneath the forward anvil.

The line-normal structure of the VHF lightning source density, which was computed over a five minute period and across a 10 km wide portion of the MCS in the line-parallel direction, was remarkably similar in each of the four vertical cross-sections (Figures 3a-d). In the convective region, the peak source density occurred in a bi-modal pattern. A broad, upper-level maximum in the VHF lightning source density was located between about 8 and 11 km AGL in the convective line. Another broad maximum in the source density was found at lower-levels in the convection from about 3 to 6 km AGL. A relative lack of VHF lightning sources existed at mid-levels (6 to 8 km) in the convective line. Narrow fingers of enhanced VHF
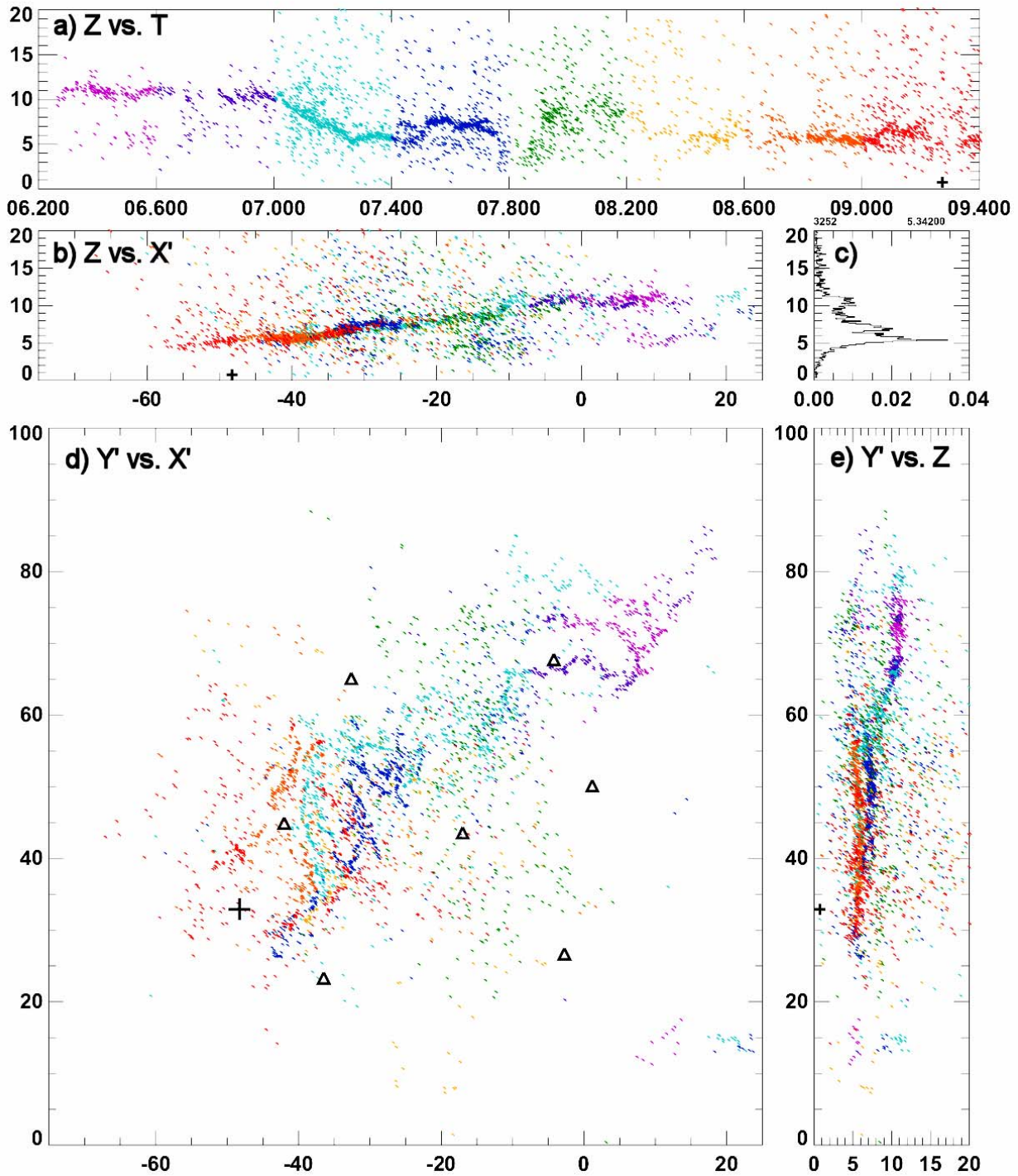
Figure 4. Depiction of an extensive LDAR II observed lightning flash that originated at about 06:20:06.2 UTC within upper levels of the convective line and extended rearward into the stratiform region, coming to ground as a NLDN-detected positive ground stroke at 06:20:09.273 UTC. Each VHF source is shown as a dot and was observed by at least five sensors of the LDAR II network. **a)** Height (Z, km) versus time (T, sec), **b)** height (Z, km) versus line-normal distance (X′, km), **c)** normalized VHF source frequency as a function of height (Z, km), **d)** line-parallel (Y′, km) versus line-normal (X′, km) distance, and **e)** line-parallel distance (Y′, km) versus height (Z, km). Each dot is color coded in time as shown in a). The plus symbol indicates the location of a single NLDN-detected positive CG lightning flash in the stratiform region that was associated with the LDAR flash (see also Figure 1 at X = 3.4 km and Y = 40.2 km or X′ = -48.3 km and Y′ = 32.9 km). The seven triangles in a) depict the location of the LDAR II network.

lightning source density bridged this mid-level gap between the bi-modal source density maxima at lower- and upper-levels.

In the convective region, the lower-level maximum in VHF lightning source density tended to follow the radar reflectivity contours, sloping slightly downward from the mature portions of the convective line to the dissipating, rear portion of the convective line. Some VHF lightning sources were located within the transition zone at low levels. In at least one cross-section (Figure 3d), the low-level source density maximum in the mature-to-dissipating convection appeared to continue its downward and rearward slant through the transition zone and into the front edge of the stratiform region. Interestingly, relatively few VHF lightning sources were located within the newest, developing-to-mature convective cells at low-to-mid levels, when compared to the mature-to-dissipating cells. This result appears to confirm the findings of Mazur and Rust (1983), who observed an overall maximum in total flash density at the rear of the convective line in a squall line system.

The upper-level VHF source density maximum in the convective region was relatively steady in altitude from about $X' = 0$ km to $X' = 25$ km. Rearward ($X' < 0$) of the mature convective line at upper levels ($Z = 9$ km AGL), the lightning source density maximum sloped downward by 4-5 km and rearward by 40-50 km along with the radar reflectivity contours, following the tops of the dissipating convective cells, across the transition zone, into the front part of the stratiform precipitation region, and terminating at the top of the bright band (just warmer than environmental $0°$C at $Z = 4.5$ km AGL). It is interesting to note that the radar reflectivity either levels out or actually slopes strongly upward over the beginning portions of the stratiform region (Figures 3a-d). The change in the slope of reflectivity in the vertical vs. line-normal plane at the leading edge of the stratiform region is likely indicative of active ice particle growth via deposition, aggregation, and possibly riming in the mesoscale updraft region [e.g., Houze and Churchill, 1984; Rutledge and Houze, 1987; Schuur and Rutledge 2000a,b]. Using the synthetic-dual-Doppler technique on KFWS data, McCormick [2003] estimated a mesoscale updraft of about 0.0 to 0.4 m s^{-1} above the stratiform bright band of the MCS on 16 June 2002. Although the lightning continued its downward and rearward slope to the stratiform bright band, there was a slight change in slope associated with an increase in the horizontal layering of VHF source density beginning at the leading edge of the stratiform precipitation (e.g., especially Figure 3b).

The distinctive slantwise pattern in the VHF source density was remarkably similar in each of the four vertical cross-sections (Figures 3a-d). In each cross-section, the sloping VHF lightning source density maximum ended at or very close to an enhanced (45 dBZ) reflectivity maximum in the bright band. Interestingly, a positive ground flash occurred (see Figure 1; $X = 3.4$ km and $Y = 40.2$ km or $X' = -48.3$ km and $Y' = 32.9$ km) during this period beneath one of these reflectivity enhancements in the stratiform region

at about $X' = -45$ km in Figure 3d (at $Y' = 31$ km), similar to the results of Rutledge and MacGorman [1988] and Rutledge and Petersen [1994]. Note that the reflectivity enhancement and the positive ground flash occurred about where the sloping VHF source density maximum terminated in the bright band (c.f. Figure 1 and 3d).

At this point, it is worthwhile to pause and investigate more carefully the apparent relationship between the NLDN-detected positive ground flash in Figure 1 and the line-normal, vertical cross-section of VHF source density in Figure 3d. To this end, the individual VHF source locations, which were detected by at least five LDAR II sensors, for the flash that produced the positive ground stroke are presented in Figures 4a-e. The LDAR II detected lightning flash began aloft ($Z = 10$ km AGL) in the rearward portion of the convective line on the northern end at $X' = 7.5$ km, $Y' = 67.5$ km (c.f. Figures 2 and 4a-e). From 06:20:06.2 UTC to 06:20:07.3 UTC (hereafter 6.2 to 7.3 seconds), the lightning flash followed a downward and rearward slanting pathway. It propagated rearwards from the convective line, through the transition zone, and to the stratiform region at $X' = -37.5$ km and downwards to just above the bright band at $Z = 5$ km (c.f. Figures 2, 3d, and 4a-e). Once at Z=5 km AGL, the flash turned abruptly left and began to travel parallel to the convective line at $X' = -37.5$ km (i.e., traveling toward the southwest). The flash propagated more than 20 km in this direction at heights between 5 km and 6 km (Figures 4d,e). Between 7.4 and 7.8 seconds, another flash segment appeared about 5 km to 10 km closer to the convective line (i.e., centered at $X' = -31$ km) and was horizontally layered at heights between 7 and 7.5 km AGL (Figures 4a,d,e). From 7.8 to 8.8 seconds, the VHF sources became noisy and spatially incoherent. Close inspection of Figure 4b suggests that many of the VHF sources during this period occurred along portions of the previously identified sloping channel in the $X' - Z$ plane. From 8.8 seconds until 9.3 seconds when the NLDN-detected a positive ground stroke, the lightning flash was more spatially coherent, spatially extensive, and horizontally layered at heights between 5 km and 6 km (e.g., Figures 4d,e). The positive ground stroke was detected by the NLDN beneath this horizontally extensive flash segment. The long-lived, spatially extensive, and horizontally stratified lightning channels (e.g., layers centered at about 5 and 7 km AGL as seen in Figures 4c-e) between 7.3 seconds and 9.3 seconds are clearly reminiscent of the "spider" lightning activity observed by Mazur et al. (1998) in stratiform precipitation as part of the intracloud component of a positive CG lightning flash.

Including the ground stroke shown in Figures 4, we conducted detailed analysis of the VHF sources associated with seven NLDN-detected positive ground strokes in the stratiform region, which occurred during the half-hour time frame of interest and within 30 km of the center of the LDAR II network, and had positive peak currents over 10 kA. For brevity, we have not shown each individual flash structure here. The detailed structure of each LDAR II lightning flash varied. Nonetheless, there were several common properties of
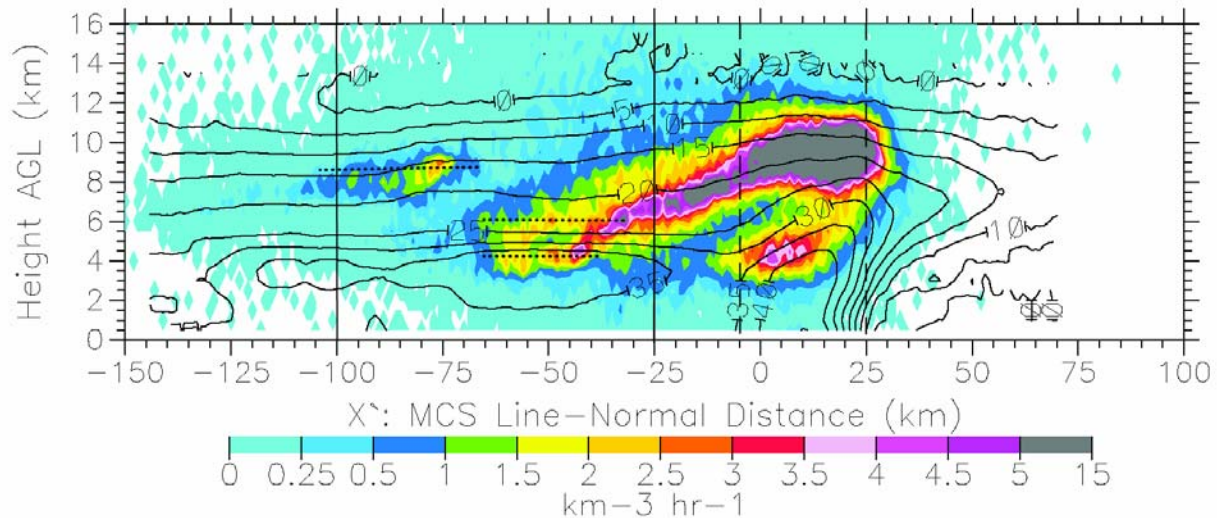
Figure 5. A 15-minute, line-normal vertical composite of radar reflectivity (dBZ, contours every 5 dBZ) and VHF lightning source density (km^{-3} hr^{-1}, shaded as shown) through a leading line, trailing stratiform MCS over the DFW region on 16 June 2002 from 0624 to 0639 UTC. The coordinate system for the composite is line-normal distance (X′, km) along the abscissa and height above ground level (AGL, km) along the ordinate. The back of the convective line (i.e., roughly the mean position of the low-level, 40 dBZ echo) was forced to be located at X′ = 0 km. To obtain the composite image, the radar reflectivity and VHF source density were averaged over the 30-minute period along the line-parallel portion of the MCS that was centered on the KFWS radar, as seen in Figure 2. The solid (dashed) vertical lines at X′ = -25 km and -100 km (-5 km and 25 km) define the domain for the line-parallel composite of the stratiform (convective) region shown in Figure 8a (8b). The dotted lines indicate the general location of quasi-horizontally layered lightning activity in the stratiform region.

the VHF sources associated with each positive ground stroke. All of the LDAR II flashes associated with the positive ground strokes were initiated in the convective line, as determined by manual inspection of VHF sources. Most (6 out of 7) of them were originated in the upper VHF maximum (8-12 km AGL) within the convective region. Even the one flash that originated in the lower VHF maximum (5 km AGL) quickly propagated to the upper convective region. All of the flashes followed a slanting pathway from the top of the convection line to the stratiform region (i.e., 35-50 km rearward and 3-5 km downward). However, the progression of VHF sources was generally not the same. In some positive CG flashes, the sloping pathway was illuminated by VHF radiation multiple times during the flash history. Once over the stratiform region, all of the positive lightning flashes were horizontally extensive, covering a total area on the order of 10^4 km^2, as in Lang et al. [2004a], and exhibited highly branched structures reminiscent of examples from past studies on "spider" lightning [e.g., Krider, 1974; Mazur et al., 1998]. The branched VHF structures illuminated completely different parts of the stratiform cloud in different horizontal layers at different times during the flash history (e.g., Figures 4). Evidence of layered lightning in the stratiform region could be determined in 3 of the LDAR II flashes associated with 4 of the 7 positive ground

strokes. As in Figure 4, the flashes often became very noisy and spatially diffuse during the "spider" lightning phase over the stratiform region. As a result, it was sometimes not possible to determine if and where the flash was occurring in horizontal layers. The lightning flash duration from first LDAR II detected VHF source to the NLDN-detected ground stroke varied from 1.4 to 3.1 seconds.

Overall, relatively fewer VHF sources occurred within the stratiform region compared to the convective region (Figures 2, 3a-d). VHF source density decreased with increasing distance rearward of the convective line. There were very few VHF sources at low levels in the stratiform region (Figures 3a-d). These trends may be partially associated with the decreased source detection efficiency of the LDAR II network with range (Appendix C), which is potentially significantly poorer at low levels (< 3 km altitude) for distant sources because of interference between direct and ground-reflected signals in the vicinity of the LDAR antennas (Terman et al 1955). However, the paucity of VHF sources in the stratiform region, particularly below 3 km height, is consistent with low CG flash density in the stratiform region of this and most other MCSs (e.g., Rutledge and MacGorman, 1988) and with generally weaker electric fields and charge densities below 3 km in stratiform precipitation (Stolzenburg et al., 1994; Lyons et al.

2003; Lang et al. 2004a). Some interesting lightning features were detected toward the rear of the stratiform region, where the LDAR flash detection efficiency was estimated to be > 90%. In Figure 3a, a horizontally oriented maximum in the VHF source density was located at upper levels (7.5 km to 10 km AGL) from $X' = -85$ km to -105 km. Another smaller, weaker grouping of VHF sources aloft occurred at about $X' = -115$ km to -120 km. Both isolated maxima toward the rear of the stratiform region were approximately 2.5 km thick and were centered at about 8.5 to 9 km AGL. Other horizontally layered lightning activity in the line-normal direction was located just above the bright band between 4 and 5 km AGL (e.g., see horizontal layers centered on $Z = 4.5$ km AGL between $X' = -35$ km and $X' = -45$ km in Figures 3b-d).

There was a relative dearth of VHF lightning sources detected in the forward anvil region shown in Figures 3a-d. Although this may be partly related to LDAR source detection efficiency issues at these ranges (50 to 100 km) as shown in Appendix C, there was clearly less lightning just forward of the convection than just to the rear of the line. One positive ground flash occurred (see Figure 1; X = 75.6 km and Y = 4.5 km) about 10 km forward of the convective line ($X' = 32$ km) in between the cross sections depicted in Figures 3a,b (or $Y' = 61$ and 51 km, respectively). More LDAR VHF sources occurred forward of the convective line ($X' > 20$) in Figures 3a,b compared to Figures 3c,d where no positive ground flashes were detected by the NLDN during this period. Careful inspection of Figure 3a and the individual flash structure (not shown) revealed that a finger of VHF sources did emanate from the convective line toward the ground flash in question, providing limited support for the convective-scale (i.e., order 10 km) tilted-dipole hypothesis [Brook et al. 1982] in the forward anvil of this MCS.

The line-normal composite (X'-Z) of vertical radar and VHF lightning source density structure during a 15-minute period from 0624-0639 UTC is given in Figure 5. The composite line-normal source density structure is remarkably similar to the individual vertical cross-sections at 0619 UTC (Figures 3a-d) and the structure of a single lightning flash (Figures 4). Furthermore, the composite radar reflectivity morphology is also very similar to the instantaneous cross-sections. This similarity across temporal and spatial scales strongly suggests that, for our mature LLTS MCS, the line-normal vertical structure of radar and lightning was quasi-steady and reasonably symmetric in the line-parallel direction. The latter conclusion will be investigated further in the next section.

In the line-normal vertical composite of radar reflectivity, the convective line was clearly evident at $-5 < X' < 30$ km. The convective line tilted forward slightly with height and gave way to the forward anvil at about $X' > 30$ km. Rearward of the convective line, the transition zone was located between about $X' = -5$

km and $X' = -20$ km. In the transition zone, the reflectivity contours began to slump noticeably downward toward the rear. As indicated by the bright band structure in the reflectivity, the stratiform region began at about $X' = -20$ km and extended to about $X' = -125$ km in the analysis domain.

Toward the rear portion of the convective line, there were two maxima of the VHF source density in the vertical, forming a lightning source density bipole. The height of the low-level maximum was located between about 3 and 6 km AGL and was centered on 4.5 km AGL. The height of the upper level maximum was centered on 9.5 AGL (8-11 km AGL) and was shifted about 7 km forward of the low-level maximum in the line-normal direction. The bi-modal distribution of VHF sources in convection at these heights is similar to past studies of convection with VHF observations [e.g., Proctor, 1991] and the related MCS lightning study by Dotzek et al. [2004]. The tilt of the vertical lightning source density bipole in the line-normal plane was accompanied by a similar forward tilt in the radar reflectivity contours, and was aligned with the 0-6 km vertical wind shear vector from the 00 UTC Dallas-Fort Worth (FWD) sounding, which was ~15 m s^{-1} from 330°. Assuming a typical updraft speed of about 10 m s^{-1}, it would have taken roughly 500 s for an air parcel to travel from the low level VHF maximum to the upper level one (i.e., 5000 m/10 m s^{-1}). Using the shear vector above, the updraft parcel would have been displaced horizontally roughly 7.5 km (i.e., 500 s ● 15 m s^{-1}) downwind during this time, in good agreement with the observed tilt. The upper level convective source density contours bulged forward of the convective line by about 10 km and downward by several km into the forward anvil region. Notice that the low-to-mid levels (0 to 7 km AGL) of the forward portions of the convective line (i.e., the forward reflectivity gradient region from $X' = 20$ to $X' = 30$ km), where the newer and often intense updrafts are typically located, were nearly devoid of VHF sources. Significantly lower lightning source densities also existed in the vertical space (6-8 km AGL) between the two lightning source maxima in the convective line but the two centers were clearly connected by a bridge of enhanced VHF source densities.

The upper level VHF source density maximum sloped downward by about 4 to 5 km and rearward of the convective line by about 40 to 50 km. Note that the downward slope of the VHF source density was similar to the downward slope of the reflectivity contours in the transition zone. The descending slope of the VHF source density decreases somewhat (i.e., becomes a bit more horizontal) over the stratiform region while the reflectivity contours level off significantly. This downward and rearward sloping lightning pathway from the upper reaches of the convective line is remarkably similar to the trajectories followed by snow particles that are detrained from the convective line, are transported rearward by the storm-relative front-to-rear (FTR) flow, descend downward through the weak mesoscale updraft

[McCormick, 2003] to the melting level because of their significantly larger fall speeds, forming the radar bright band, and then fall to the ground as stratiform rainfall [e.g., Houze et al., 1989; Figure 9]. As shown in Dotzek et al. [2004], a surprisingly similar sloping lightning structure rearward of the convective line was found in our analysis of the 7-8 April 2002 MCS in Texas.
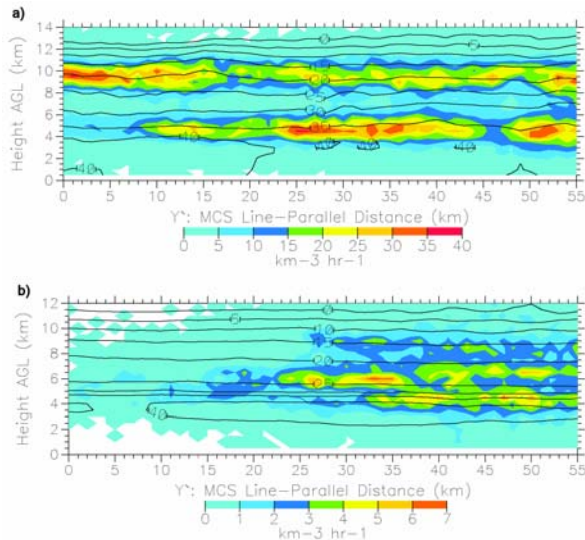
Figure 6. Fifteen minute, line-parallel vertical composites of radar reflectivity (dBZ, contours every 5 dBZ) and VHF lightning source density (km^{-3} hr^{-1}, shaded as shown) through a leading line, trailing stratiform MCS over the DFW region on 16 June 2002 for the **a)** convective region from 0609-0624 UTC and the **b)** stratiform region from 0624-0639 UTC. Notice the factor of 5 decrease in scale of the VHF source density shading from a) to b). The coordinate system for the composite is line-parallel distance (Y′, km) along the abscissa and height above ground level (AGL, km) along the ordinate. The compositing domains for the two regions are highlighted in Figure 5.

A separate, horizontally layered VHF lightning source density maximum was located at upper levels (7-10 km AGL) further rearward in the stratiform region from about X′ = -65 km to X′ = -110 km in Figure 5. This separate lightning zone at the back of the stratiform region was also noted in Figure 3a. The VHF source densities in this secondary maximum at the rear of the stratiform region were significantly less than in the convective region VHF maxima or in the downward and rearward sloping VHF maxima in the forward portions of the stratiform region. Nonetheless, this horizontally oriented lightning zone was a fairly persistent feature of the MCS stratiform region and was observed despite being located about 40 to 85 km from the center of the LDAR II network. There were also horizontally stratified lightning layers centered at both 4 km and 6 km AGL that intersected the slanted lightning pathway over the bright band.

As a result, the slopes of radar reflectivity and VHF source density were closely matched in the stratiform precipitation region of Figure 5 (i.e., both became quasi-horizontal). The lightning layer centered at 4 km was located below the environmental melting level (i.e., T=0°C was at 4.8 km AGL according to FWD 0000 UTC sounding). The environmental temperature from the same sounding associated with the stratified VHF source activity centered at 6 km was about -11°C.

3.4 Line-Parallel Vertical Radar and Total Lightning Structure

Line-parallel composites of the radar reflectivity and VHF source density for the convective and stratiform regions are shown in Figures 6a and 6b, respectively. As seen earlier, the convective region lightning activity formed a bipole pattern in the vertical with VHF source density maxima located at low levels from 3 km to 6 km and at upper levels from 8 km to 11 km (Figure 6a). A relative minimum in VHF source density was located in between the two maxima from 6 km to 8 km. Within the upper and lower lightning layers, there was obvious along line variability in the VHF source density. As expected for a squall line, there were local maxima in the lightning activity along the line that were associated with individual convective cells.

As noted earlier, VHF source densities in the stratiform region were a factor of 5 to 10 less than in the convective region (c.f. Figures 6a and 6b). Line-parallel composite lighting activity in the stratiform region was also horizontally stratified but a bit more complex than in the convective zone. As seen in Figure 6b, there are at least three horizontal layers of VHF source density that occurred approximately from 1) 3.5 km to 5 km AGL (FWD/00 UTC: 7°C to -2°C), 2) 5.5 km to 7.5 km AGL (-6°C to -19°C), and 3) 8 km to 10 km AGL (-22°C to -39°C). There was along line variability in the presence and exact height of these layers. Either because of real along line variability in stratiform region properties or, more likely, because of the low VHF source densities in the stratiform region and decreasing detection efficiency with range from the center of the network (Y′ = 44 km), the LDAR II network did not observe as much layered lightning activity in the southern portions of the stratiform region. From Y′ = 38 km to 55 km, the middle layer was centered at 6.5 km. From Y′ = 22 km to 37 km, the middle layer was shifted lower with a center at 6 km. Individual lightning flashes within the stratiform region stratified into more narrow ranges of heights within these three composite layers. For example, the lightning flash highlighted in Figures 4 and 5 exhibited extensive layering centered at both 5 km and 7 km, corresponding to the lower and middle layers identified in Figure 6b. Even within the three layers, there was along line variability (i.e., local maxima) in the stratiform region (Figure 6b). Due to low flash rates, this variability within the fifteen minute composite still represents the line-parallel behavior of individual lightning flashes within the stratiform region

such as in Figures 4 and 5. Given a much longer sample of the stratiform region over the center of the LDAR II network, it is not clear whether this along line variability would persist.

4. SUMMARY AND CONCLUSIONS

Horizontal and line-normal, vertical cross-sections and composite images of Dallas-Fort Worth Lightning Detection and Ranging (LDAR II) VHF radiation sources and radar reflectivity over a 30-minute period provide a unique perspective on lightning pathways within a leading-line, trailing-stratiform (LLTS) mesoscale convective system (MCS) on 16 June 2002. The overwhelming majority of VHF lightning sources occurred within the leading convective line in a bi-modal pattern in the vertical. Assuming that VHF source density maxima were most likely associated with positive charge, then the LDAR II observations suggest that the gross charge structure of the convective region of the MCS was characterized by a tripole with net positive charge centered at 4.5 km AGL (3°C) and 9.5 km AGL (-35°C) and net negative charge centered roughly in the relative minimum of the VHF source density maximum at 7 km AGL (-17°C). A persistent lightning pathway and inferred positive charge zone sloped rearward (by 40-50 km) and downward (by 4-5 km) from the upper VHF source maximum in the convective line, through the transition zone, and into the radar bright band of the stratiform region. In the stratiform region, VHF lightning sources and inferred positive charge were concentrated in three layers centered at 4.5, 6, and 9 km AGL (2°C, -11°C, and -31°C, respectively), consistent with past electric field studies of symmetric LLTS MCSs.

Positive cloud-to-ground lightning flashes in the stratiform region were initiated in the convective line and followed the slanting pathway from the top of convective cores to the stratiform precipitation, where they were horizontally extensive, layered, and highly branched. The sloping lightning pathway was identical to hypothetical trajectories taken by snow particles. These observations provide further support for the advection of charge on snow along the sloping pathway and the in-situ generation of charge in the horizontal lightning layers as primary contributors to electrification and positive lightning production rearward of the convective line.

6. REFERENCES

Boccippio, D. J., The electrification of stratiform anvils, Ph.D. Dissertation, Massachusetts Institute of Technology, 1996.

Boccippio, D.J., S.J. Heckman, and S.J. Goodman, A diagnostic analysis of the Kennedy Space Center LDAR network. 1. Data characteristics, *J. Geophys. Res.*, **106**, 4769-4786, 2001.

Brook, M., M. Nakano, P. Krehbiel, and T. Takeuti, The electrical structure of the Hokuriku winter thunderstorms, *J. Geophys. Res.*, **87**, 1207-15, 1982.

Coleman, L.M., T.C. Marshall, M. Stolzenburg, T. Hamlin, P.R. Krehbiel, W. Rison, and R.J. Thomas, Effects of charge and electrostatic potential on lightning propagation, *J. Geophys. Res.*, **108**(D9), 4298, doi:10.1029/2002JD002718, 2003.

Cressman, G., An operational analysis system, *Mon. Wea. Rev.,* **87**, 367-374, 1959.

Crum, T. D., R. L. Alberty, and D. W. Burgess, Recording, archiving, and using WSR-88D data, *Bull. Amer. Meteor. Soc.,* **74,** 645-653, 1993.

Cummins, K. L., M. J. Murphy, E. A. Bardo, W. L. Hiscox, R. B. Pyle, and A. E. Pifer, A combined TOA/MDF technology upgrade of the U.S. National Lightning Detection Network, *J. Geophys. Res.*, **103**, 9035 – 9044, 1998.

Dotzek, N., R. M. Rabin, L. D. Carey, D. R. MacGorman, T. L. McCormick, N. W. Demetriades, M. J. Murphy, and R. L. Holle, Lightning activity related to satellite and radar observations of a mesoscale convective system over Texas on 7-8 April 2002, *Atmos. Res.*, **accepted pending revisions**, 2004.

Engholm, C. D., E. R. Williams, and R. M. Dole, Meteorological and electrical conditions associated with positive cloud-to-ground lightning, *Mon. Wea. Rev.,* **118,** 470-487, 1990.

Fritsch, J. M., and G. S. Forbes, Mesoscale Convective Systems, *Severe Convective Storms*, Ed. C. A. Doswell, III, Meteorological Monographs, Vol. 28, No. 50, Amer. Meteor. Soc., 323-358, 2001.

Fritsch, J. M., R. J. Kane, and C. R. Chelius, The contribution of mesoscale weather systems to the warm-season precipitation in the United States, *J. Climate Appl. Meteor.*, **25**, 1333-1345, 1986.

Goodman, S. J., and D. R. MacGorman, Cloud-to-ground lightning activity in mesoscale convective complexes, *Mon. Wea. Rev.*, **114**, 2320-2328, 1986.

Hobbs, P. V., S. Chang, and J. D. Locatelli, The dimensions and aggregation of ice crystals in natural cloud. *J. Geophys. Res.*, **79**, 2199-2206.

Holle, R. L., A. I. Watson, R. E. Lopez, and D. R. MacGorman, The life cycle of lightning and severe weather in a 3-4 June 1985 PRE-STORM mesoscale convective system, *Mon. Wea. Rev.*, **122**, 1798-1808, 1994.

Houze, R. A. Jr., *Cloud dynamics*, Academic Press, San Diego, 573 pp., 1993.

Houze, R. A. Jr., and D. D. Churchill, Microphysical structure of winter monsoon cloud clusters, *J. Atmos. Sci.*, **41**, 3405-3411.

Houze, R. A. Jr., S. A. Rutledge, M. I. Biggerstaff, and B. F. Smull, Doppler radar depiction of midlatitude mesoscale convective systems, *Bull. Am. Meteorol. Soc., 70*, 608-619, 1989.

Houze, R. A. Jr., B. F. Smull, and P. Dodge, Mesoscale organization of springtime rainstorms in Oklahoma, *Mon. Wea. Rev.*, **117**, 613-654, 1990.

Hunter, S. H., T. J. Schuur, T. C. Marshall, and W. D. Rust, Electric and kinematic structure of the Oklahoma mesoscale convective system of 7 June 1989, *Mon. Wea. Rev.*, **120**, 2226-2239, 1992.

Krehbiel, P. R., The electrical structure of thunderstorms. *The Earth's Electrical Environment, Studies in Geophysics,* National Academy Press, 90-113, 1986.

Krehbiel, P. R., R. J. Thomas, W. Rison, T. Hamlin, J. Harlin, and M. Davis, GPS-based mapping system reveals lightning inside storms, *Eos Trans., 81*, 21-25, 2000.

Krider, R. P., An unusual photograph of an air lightning discharge, *Weather*, **29**, 24-27, 1974.

Lang, T. J., S. A. Rutledge, and K. C. Wiens, Origins of positive cloud-to-ground lightning flashes in the stratiform region of a mesoscale convective system. *Geophys. Res. Lett.*, 31, L10105, doi:10.1029/2004GL019823, 2004a.

Lang, T. J., et al., The Severe Thunderstorm Electrification and Precipitation Study (STEPS), *Bull. Amer. Meteorol. Soc.*, in press, 2004b.

Lennon, C., and L. Maier, Lightning mapping system, Proceedings of the International Aerospace and Ground Conference on Lightning and Static Electricity, Cocoa Beach, FL, NASA Conference Publication 3106, Vol. II, 89.1-89.10, 1991.

Ligda, M. G. H., The radar observation of lightning, *J. Atmos. Terr. Phys.*, **9**, 329-346.

Locatelli, J. D., and P. V. Hobbs, Fall speeds and masses of solid precipitation particles, *J. Geophys. Res.*, **79**, 2185-2197, 1974.

Lyons, W. A., E. R. Williams, S. A. Cummer, M. A. Stanley, Characteristics of sprite-producing positive cloud-to-ground lightning during the19 July 2000 STEPS mesoscale convective systems, *Mon. Wea. Rev.*, **131**, 2417-2427.

MacGorman, D. R., and W. D. Rust, *The Electrical Nature of Storms*, Oxford Univ. Press, New York, 422 pp., 1998.

MacGorman, D. R., and C. D. Morgenstern, Some characteristics of cloud-to-ground lightning in mesoscale convective systems, *J. Geophys. Res.*, **103**, 14,011-14,023, 1998.

MacGorman, D. R., A. A. Few, and T. L. Teer, Layered lightning activity, *J. Geophys. Res.*, **86**, 9900-9910, 1981.

Maier, L., C. Lennon, T. Britt, and S. Schaefer, Lightning Detection and Ranging (LDAR) system performance analysis, 1995 Int'l Conf. on Cloud Physics, Dallas, Texas, Amer. Meteorol. Soc., 1995.

Marshall, T. C., and W. D. Rust, Two types of vertical electrical structures in stratiform precipitation regions of mesoscale convective systems, *Bull. Amer. Meteorol. Soc.*, **74**, 2159-2170, 1993.

Marshall, T. C., M. Stolzenburg, W. D. Rust, Electric field measurements above mesoscale convective systems, *J. Geophys. Res.*, **101**, 6979-6996, 1996.

Mazur, V., and W. D. Rust, Lightning propagation and flash density in squall lines as determined with radar, *J. Geophys. Res.*, **88**, 1495-1502, 1983.

Mazur, V., and L.H. Ruhnke, Common physical processes in natural and artificially triggered lightning, *J. Geophys. Res.*, **98**, 12913-12930, 1993.

Mazur, V., E. Williams, R. Boldi, L. Maier, and D.E. Proctor, Initial comparison of lightning mapping with operational time-of-arrival and interferometric systems, *J. Geophys. Res.*, **102**, 11071-11085, 1997.

Mazur, V., X-M Shao, and P. R. Krehbiel, "Spider" lightning in intracloud and positive cloud-to-ground flashes, J. Geophys. Res., 103, 19811-19822, 1998.

McCormick, T. L, *Three-dimensional radar and total lightning characteristics of mesoscale convective systems,* M.S. thesis, Dept. of Marine, Earth, and Atmos. Sci., North Carolina State Univ., [Available online at http://www.lib.ncsu.edu/theses/available/etd-08042003-035751/unrestricted/etd.pdf], 354 pp., 2003.

Mo, Q., A. G. Detwiler, J. Hallett, and R. Black, Horizontal structure of the electric field in the stratiform region of an Oklahoma mesoscale convective system, *J. Geophys. Res.*, **108**, D7, 4225, doi:10.1029/2001JD001140, 2003.

Orville, R. E., R. W. Henderson, and L. F. Bosart, 1988: Bipole patterns revealed by lightning locations in mesoscale storm systems, *Geophys. Res. Lett.*, **15**, 129-132, 1988.

Oye, D., and M. Case, *REORDER: A program for gridding radar data. Installation and use manual for the UNIX version,* NCAR Atmospheric Technology Division, Boulder, CO, 1995.

Petersen, W. A., and S. A. Rutledge, Some characteristics of cloud-to-ground lightning in tropical northern Australia, *J. Geophys. Res.*, **97**, 11,553-11,560, 1992.

Proctor, D. E., A hyperbolic system for obtaining VHF radio pictures of lightning, *J. Geophys. Res.*, **76**, 1478-1489, 1971.

Proctor, D. E., Regions where lightning flashes began, *J. Geophys. Res.*, **96**, 5099-5112, 1991.

Rison, W., R.J. Thomas, P.R. Krehbiel, T. Hamlin, and J. Harlin, A GPS-based three-dimensional lightning mapping system: Initial observations in central New Mexico, *Geophys. Res. Lett.*, **26**,

3573-3576, 1999.

Rutledge, S. A., and R. A. Houze Jr., A diagnostic modeling study of the trailing stratiform region of a midlatitude squall line, *J. Atmos. Sci.*, **44**, 2640-2656, 1987.

Rutledge, S. A., and D. R. MacGorman, Cloud-to-ground lightning activity in the 10-11 June 1985 mesoscale convective system observed during the Oklahoma-Kansas PRE-STORM project, *Mon. Wea. Rev.,* **116**, 1393-1408, 1988.

Rutledge, S. A., and W. A. Petersen, Vertical radar reflectivity structure and cloud-to-ground lightning in the stratiform region of MCSs: Further evidence for in situ charging in the stratiform region, *Mon. Wea. Rev.*, **122**, 1760-1776, 1994.

Rutledge, S. A., C. Lu, and D. R. MacGorman, Positive cloud-to-ground lightning flashes in mesoscale convective systems, *J. Atmos. Sci.*, **47**, 2085-2100, 1990.

Rutledge, S. A., E. R. Williams, and W. A. Petersen, Lightning and electrical structure of mesoscale convective systems, *Atmos. Res.*, **29**, 27-53.

Saunders, C. P. R., W. D. Keith, and R. P. Mitzeva, The effect of liquid water on thunderstorm charging, *J. Geophys. Res., 96*, 11,007-11,017, 1991.

Schuur, T. J., B. F. Smull, W. D. Rust, and T. C. Marshall, Electrical and kinematic structure of the stratiform precipitation region trailing an Oklahoma squall line, *J. Atmos. Sci.*, **48**, 825-842, 1991.

Schuur, T. J., and S. A. Rutledge, Electrification of stratiform regions in mesoscale convective systems, Part I: An observational comparison of symmetric and asymmetric MCSs, *J. Atmos. Sci.,* **57**, 1961-1982, 2000a.

Schuur, T. J., and S. A. Rutledge, Electrification of stratiform regions in mesoscale convective systems, Part II: Two-dimensional numerical model simulations of a symmetric MCS, *J. Atmos. Sci.*, **57**, 1983-2006, 2000b.

Shao, X. M. and P. R. Krehbiel, The spatial and temporal development of intracloud lightning, *J. Geophys. Res.,* **101**, 26,641-26,668, 1996.

Shepherd, T. R., W. D. Rust, and T. C. Marshall, Electric fields and charges near 0°C in stratiform clouds, Mon. Wea. Rev., 124, 919-938, 1996.

Stolzenburg, M., Characteristics of the bipolar pattern of lightning locations observed in 1988 thunderstorms. *Bull Amer. Meteor. Soc.*, **71**, 1331-1338, 1990.

Stolzenburg, M., T. C. Marshall, W. D. Rust, B. F. Smull, Horizontal distribution of electrical and meteorological conditions across the stratiform region of a mesoscale convective system, *Mon. Wea. Rev.*, **122**, 1777-1797, 1994.

Stolzenburg, M., W. D. Rust, B. F. Smull, and T. C. Marshall, Electrical structure in thunderstorm convective regions 1. Mesoscale convective systems, *J. Geophys. Res.*, **103**, 14,059-14,078, 1998.

Stolzenburg, M., T. C. Marshall, and W. D. Rust, Serial soundings of electric field through a mesoscale convective system, *J. Geophys. Res.*, **106**, 12,371-12,380, 2001.

Takahashi, T., Riming electrification as a charge generation mechanism in thunderstorms, *J. Atmos. Sci.,* **35,** 1536–1548, 1978.

Teer, T. L., and A. A. Few, Horizontal lightning, *J. Geophys. Res.*, **79**, 3436-3441, 1974.

Terman, F. E., R.A. Helliwell, J.M. Pettit, D.A. Watkins, W.R. Rambo, *Electronic and Radio Engineering*, 4th Ed., McGraw-Hill, New York, 1078 pp., 1955.

Thomas, R., W. Winn, S. Hunyady, W. Rison, P. Krehbiel, T. Hamlin, J. Harlin, Accuracy of the lightning mapping array, 17th Int'l. Lightning Detection Conf., Tucson, Ariz., Vaisala, Inc., 2002.

Thomas, R.J., P.R. Krehbiel, W. Rison, T. Hamlin, J. Harlin, and D. Shown, Observations of VHF source powers radiated by lightning, *Geophys. Res. Lett.*, **28**, 143-146, 2001.

Toracinta, E. R., K. I. Mohr, E. J. Zipser, and R. E. Orville, A comparison of WSR-88D reflectivities, SSM/I brightness temperatures, and lightning for mesoscale convective systems in Texas. Part I: Radar reflectivity and lightning, *J. Appl. Meteor.*, **35**, 902-918, 1996.

Wacker, R. S., and R. E. Orville, Changes in measured lightning flash count and return stroke peak current after the 1994 U.S. National Lightning Detection Network upgrade. 1. Observations, *J. Geophys. Res.,* **104,** 2151–2158, 1999a.

Wacker, R. S., and R. E. Orville, Changes in measured lightning flash count and return stroke peak current after the 1994 U.S. National Lightning Detection Network upgrade. 2. Theory, *J. Geophys. Res.,* **104,** 2159–2162, 1999b.

Williams, E. R., C. M. Cooke, and K. A. Wright, Electrical discharge propagation in and around space charge clouds, *J. Geophys. Res., 90*, 6,059-6,070, 1985.

Williams, E. R., The tripole structure of thunderstorms, *J. Geophys. Res.*, **90**, 6013-25, 1989.